



PERFORMANCE IMPROVEMENT OF A TYPE OF MILLING MACHINES

Mikho Mikhov, Marin Zhilevski

Technical University of Sofia, Sofia, BULGARIA

E-mail: mikhov@tu-sofia.bg

Summary: Problems in modernization of a type of milling machines are discussed in this paper. Two additional controlled axes are applied, namely a table rotation (axis 4) and tilting of this table (axis 5). The machines under consideration are attributed to those with multi-coordinate electric driving systems. The main requirements for the drive characteristics of each coordinate axis are formulated. A number of models for computer simulation with various electric drives have been developed aiming at studying their dynamic and static regimes for the respective control algorithms. The experimental research carried out confirms good performance of the electric drives applied. The results of this study can be used in the design and set up of such multi-coordinate driving systems.

Keywords: milling machine, modernization, additional coordinate axes, multi-coordinate driving system, performance improvement

1. INTRODUCTION

Milling machines are widely used and there is a big variety of their models and ways of practical implementation.

For modernization of a type of milling machines two additional controlled axes have been applied, namely a table rotation as axis 4 and rotary table tilting as axis 5. The goal is to extend the capabilities of these machines to process more complex machine parts and to enhance their performance. In this way, the machines under consideration can be attributed to those with multi-coordinate electric driving systems.

The corresponding electric drives in this case are as follows: 1 – for x coordinate axis; 2 – for y coordinate axis; 3 – for z coordinate axis; 4 – for rotary table; 5 – for tilting of the rotary table; 6 – for spindle.

Various electric drives [1], [2], [3], [4], [5], [6] are analyzed to choose appropriate solutions meeting the static and dynamic characteristics of the respective machine coordinates.

Electric drives for some coordinate axes have been studied by means of computer simulation and experimental research in [7], [8], [9], [10], [11], [12], [13].

The problems in modernization of the considered machines are presented in [14].

In this paper the main requirements to the necessary multi-coordinate drive system for all controlled axes are formulated. Comparative study of different solutions with DC and AC motors has been carried out aiming at performance improvement. Appropriate control programs have been developed to coordinate the coordinate axes of the machine under consideration.

Simulation and experimental results from the research carried out are presented and discussed.

2. FEATURES OF THE MULTI-COORDINATE DRIVING SYSTEM

A simplified block diagram of the multi-coordinate driving system under consideration is shown in Fig. 1. The notations are as follows: DPC – digital program control device; ED1 - ED6 – electric drives; G1 - G6 – mechanical gears; L1 - L6 – loads.

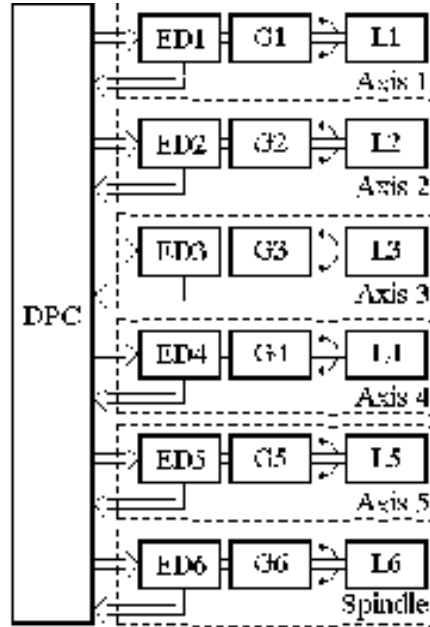


Figure 1: Block diagram of the driving system.

The coefficients of the respective mechanical gears are as follows:

$$\begin{aligned} K_{g_1} &= K_{g_2} = K_{g_3} = 10 \text{ mm/rev} \approx 1.6 \times 10^{-3} \text{ m/rad}; \\ K_{g_4} &= 2^0/\text{rev} \approx 0.00556; \\ K_{g_5} &= 3^0/\text{rev} \approx 0.00833; \\ K_{g_6} &= 1. \end{aligned} \quad (1)$$

2.1. Two coordinate *x-y* driving

The set of achievements required for the two-coordinate *x-y* drive can be formulated as follows:

- formation of the necessary motion trajectories at given position cycles;
- maximum starting torque to ensure good dynamics;
- reversible speed and torque control;
- compensation of disturbances.

The vector-matrix model of the DC electric drives used is as follows:

$$\begin{bmatrix} \frac{d\theta_i}{dt} \\ \frac{d\omega_i}{dt} \\ \frac{di_{a_i}}{dt} \end{bmatrix} = \begin{bmatrix} 0 & 1 & 0 \\ 0 & 0 & -\frac{K_{t_i}}{J_i} \\ 0 & -\frac{K_{e_i}}{L_{a_i}} & -\frac{R_{a_i}}{L_{a_i}} \end{bmatrix} \begin{bmatrix} \theta_i \\ \omega_i \\ i_{a_i} \end{bmatrix} + \begin{bmatrix} 0 \\ 0 \\ \frac{K_{c_i}}{L_{a_i}} \end{bmatrix} v_i + \begin{bmatrix} 0 \\ -\frac{1}{J_i} \\ 0 \end{bmatrix} i_{l_i}, \quad (2)$$

where: θ_i is angular position for the respective i axis; ω_i – angular speed; i_{a_i} - armature current;

K_{e_i} - back EMF voltage coefficient; K_{t_i} - torque coefficient; R_{a_i} - armature circuit resistance; L_{a_i} - armature inductance; K_{c_i} - amplifier gain of the chopper; v_i - input control signal of the power converter; J_i - total inertia referred to the motor shaft; i_{l_i} - armature current which is determined by the respective load torque; $i = 1, 2$ – number of the coordinate axes.

Detailed experimental studies have been carried out for different solutions. The following algorithms for two-coordinate position control have been realized and analyzed (Fig. 2): consecutive motion along the axes; simultaneous motion along the axes; combined motion along the axes. The notations used are as follows: S_i – linear position for the respective i axis; S_{if} – linear final position for the respective i axis.

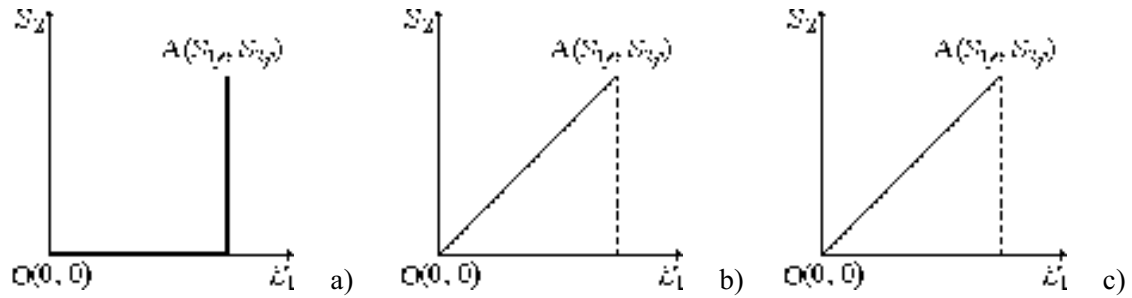


Figure 2: Motion trajectories for two-coordinate position control.

Figure 2a shows a trajectory obtained by successive movement along the coordinate axes. The total time for positioning is as follows:

$$t_p = t_{p1} + t_{p2}, \quad (3)$$

Figure 2b represents a trajectory obtained by simultaneous movement along both coordinate axes. In such way of control position time is:

$$t_p = t_{p1} = t_{p2}. \quad (4)$$

Figure 2c shows a trajectory obtained at combined motion along the coordinate axes. If both drives work at the same speeds, the total time of positioning is equal to the time necessary for the drive with longer displacement time set.

$$t_p = t_{p1}. \quad (5)$$

Some time-diagrams illustrating the drive performance are presented in Fig. 3, where V_i is linear speed for the respective i axis.

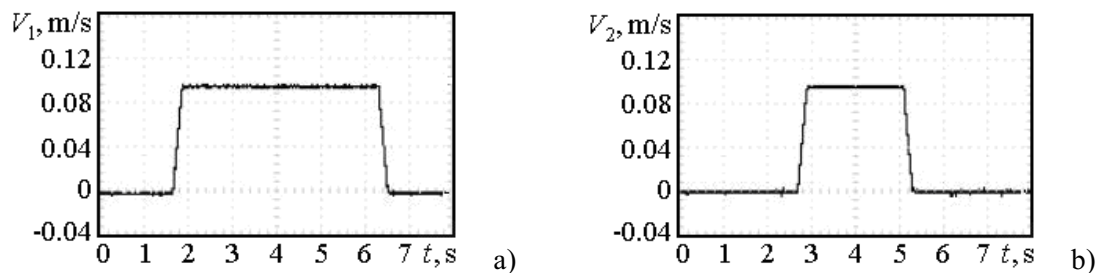


Figure 3: Speed oscillograms for the two coordinate x-y axes.

Fig. 3a shows a linear speed trajectory, obtained experimentally for displacement of 0.62 m along the x coordinate axis. A linear speed diagram, obtained for motion along the y coordinate axis is presented

in Fig. 3b. The set distance in this case is 0.32 m.

2.2. Driving of the z coordinate axis

The main requirements for the drive are as follows:

- maximum starting torque to ensure good dynamics;
- reversible speed;
- position accuracy.

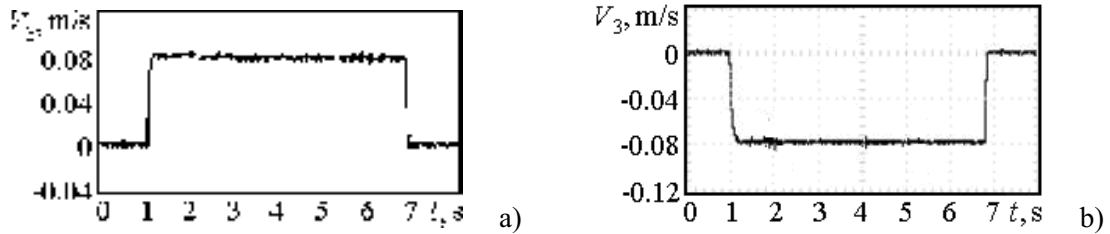


Figure 4: Speed oscillograms for the z coordinate axis.

In Figure 4 experimentally obtained time-diagrams are presented for displacements of 0.25 m along the z coordinate axis in forward and back directions, respectively.

2.3. Rotary table driving

The set of requirements for this drive can be formulated as follows:

- formation of the necessary motion trajectories at given position cycles;
- maximum starting torque to ensure good dynamics;
- reversible speed and torque control;
- compensation of disturbances.

The transfer function of the position controller applied is expressed by the following equation [6]:

$$G_{pc}(s) = \frac{2K_{sf}\varepsilon_{d\max}}{K_{pf}\omega_{\text{rat}}}, \quad (6)$$

where: K_{sf} is gain of the speed feedback; $\varepsilon_{d\max}$ – maximum deceleration; K_{pf} – gain of the position feedback; ω_{rat} – rated angular speed.

Time-diagrams presenting the performance of this electric drive are shown in Fig. 5.

Figure 5a presents an oscillogram of angular speed when the motion trajectory includes acceleration, pre-set value and deceleration. In Fig. 5b an angular speed trajectory is shown, including acceleration and deceleration when a small motion is performed.

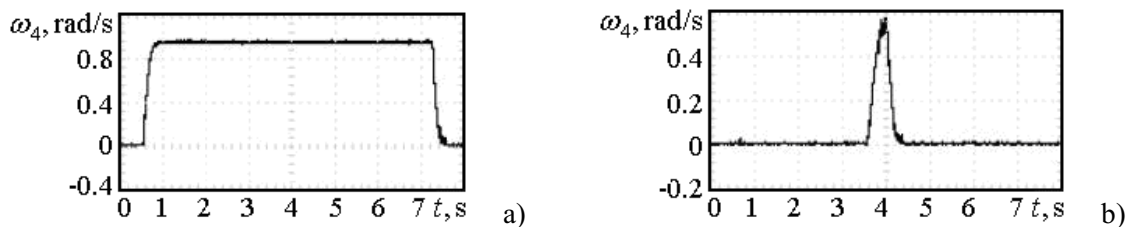


Figure 5: Angular speed oscillograms for rotary table.

Options for performance improvement through replacement of DC motor drive with permanent magnet synchronous motor (PMSM) drive have been studied. The control is carried out by rotor angular position in brushless DC motor mode [15].

The vector-matrix model of such an electric drive is described as follows:

$$\begin{bmatrix} v_a \\ v_b \\ v_c \end{bmatrix} = \begin{bmatrix} R_s & 0 & 0 \\ 0 & R_s & 0 \\ 0 & 0 & R_s \end{bmatrix} \begin{bmatrix} i_a \\ i_b \\ i_c \end{bmatrix} + \begin{bmatrix} L_a & L_{ba} & L_{ca} \\ L_{ba} & L_b & L_{cb} \\ L_{ca} & L_{cb} & L_c \end{bmatrix} \frac{d}{dt} \begin{bmatrix} i_a \\ i_b \\ i_c \end{bmatrix} + \begin{bmatrix} e_a \\ e_b \\ e_c \end{bmatrix} \quad (7)$$

where: v_a, v_b, v_c are voltages applied on the stator phases a, b and c respectively; i_a, i_b, i_c – phase currents; R_s – stator phase resistance; L_a, L_b, L_c – phase self inductances; L_{ba}, L_{ca}, L_{cb} – mutual inductances; e_a, e_b, e_c – back EMF voltages.

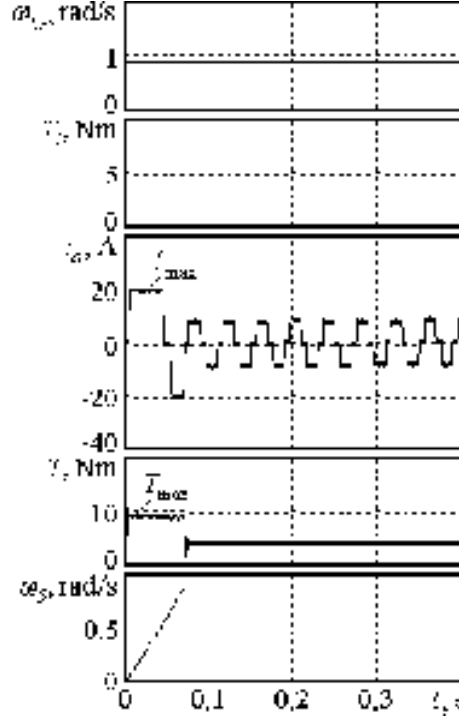


Figure 6: Starting process with current limitation.

Figure 6 presents some time-diagrams illustrating the drive performance.

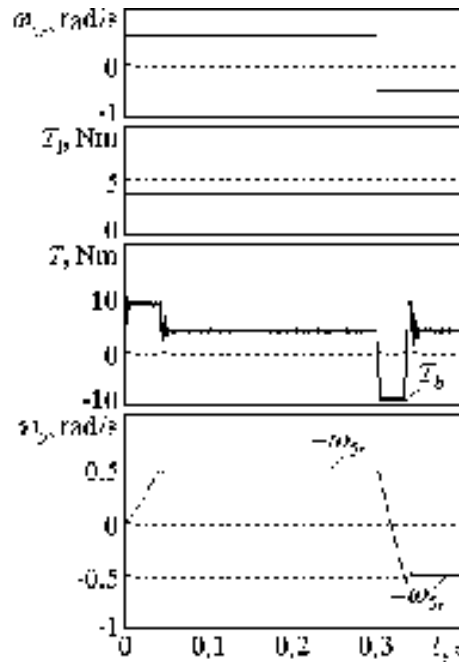


Figure 7: Reversing with electrical braking.

The reference motor speed ω_{5r} , load torque T_l , phase current i_a , motor torque T and motor speed ω_5 are shown. In this case the motor current is limited to the maximum admissible value I_{\max} which provides maximum starting motor torque T_{\max} .

Time-diagrams obtained for reverse speed control with electrical braking are shown in Fig. 7, where T_b is the braking torque.

2.4. Tilting of the rotary table

The main requirements for the respective drive can be formulated as follows:

- positioning with necessary accuracy;
- maximum starting torque to ensure good dynamics;
- reversible speed control.

Figure 8 presents some experimentally obtained time-diagrams for tilting of the rotary table of $+90^\circ$ (a) and $+60^\circ$ (b), respectively.

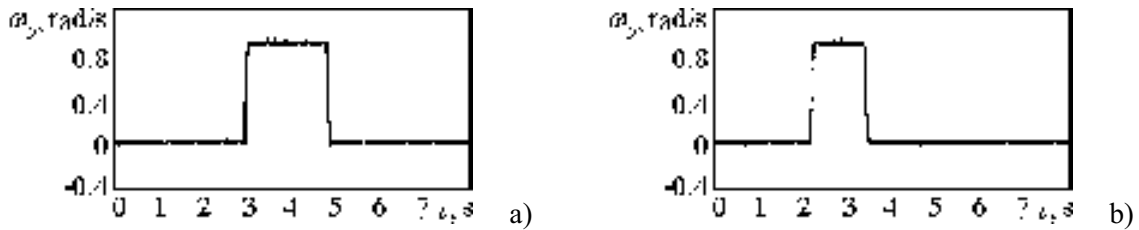


Figure 8: Speed oscillograms for tilting of the rotary table.

Some options for performance improvement through replacement of DC motor electric drive of this coordinate axis with hybrid step motor drive are analyzed.

The state-space model of the hybrid stepping drive as required for computer simulation, is as follows:

$$\begin{bmatrix} \dot{i}_a \\ \dot{i}_b \\ \dot{\omega} \\ \dot{\theta} \end{bmatrix} = \begin{bmatrix} -\frac{R}{L} & 0 & \frac{K_t}{J} \sin(p\theta) & 0 \\ 0 & -\frac{R}{L} & -\frac{K_t}{J} \cos(p\theta) & 0 \\ -\frac{K_t}{J} \sin(p\theta) & \frac{K_t}{J} \cos(p\theta) & -\frac{C}{J} & 0 \\ 0 & 0 & 1 & 0 \end{bmatrix} \begin{bmatrix} i_a \\ i_b \\ \omega \\ \theta \end{bmatrix} + \begin{bmatrix} \frac{1}{L} & 0 & 0 & 0 \\ 0 & \frac{1}{L} & 0 & 0 \\ 0 & 0 & \frac{1}{L} & 0 \\ 0 & 0 & 0 & 0 \end{bmatrix} \begin{bmatrix} v_a \\ v_b \\ T \\ 0 \end{bmatrix}, \quad (6)$$

where: v_a and v_b are phase voltages; i_a and i_b – phase currents; θ – rotor angular position; $\omega = d\theta/dt$ – motor velocity; T – motor torque; K_t – torque constant; R – stator winding resistance; L – winding inductance; p – number of the rotor teeth; J – total inertia referred to the motor shaft; C – coefficient of viscous friction.

The control is realized in microstepping mode of operation. Subdivision of the basic motor step is possible by proportioning the phase currents in the two windings (Fig. 9).

The phase currents magnitudes are calculated as follows [16]:

$$i_a(N_i) = I_{\text{rat}} \cos(\alpha_{\mu}); \quad (9)$$

$$i_b(N_i) = I_{\text{rat}} \sin(\alpha_{\mu}), \quad (10)$$

where: I_{rat} is rated phase current; N_i – number of current levels ($i = 0, 1, 2, \dots, k-1$); α_{μ} – angular

displacement of each micro-step.

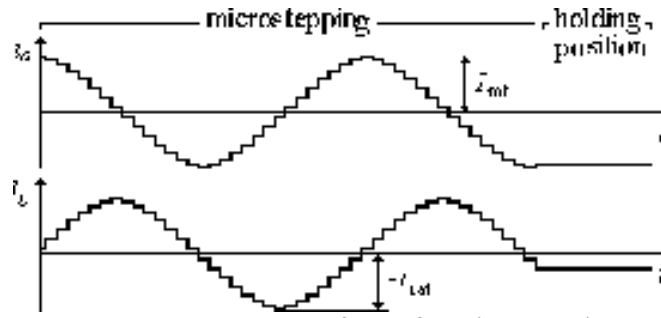


Figure 9: Current waveforms for microstepping.

The respective current vector diagram is shown in Fig. 10.

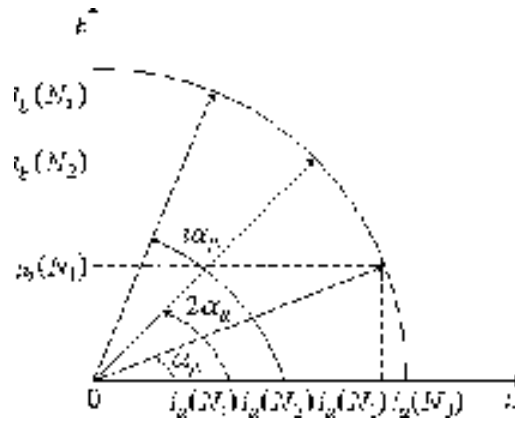


Figure 10: Vector diagram.

The resultant stator current represents the phase currents vector sum:

$$I = \sqrt{[I_{\text{rat}} \cos(i\alpha_{\mu})]^2 + [I_{\text{rat}} \sin(i\alpha_{\mu})]^2} = I_{\text{rat}}. \quad (11)$$

In this control mode the full step length is divided electronically into small increments of rotor motion:

$$\alpha_{\mu} = \alpha/k, \quad (12)$$

where: α is full step; k – number of the micro-steps in one full step.

For conventional operation modes the equilibrium positions are defined by alignment of the stator and rotor teeth and therefore are independent of the current levels. However, the micro-step positions are critically dependent on current levels in the phase windings. Hence, there is a need for closed-loop current control to ensure the respective phase current levels.

Tuning of the control system is carried out in the following sequence:

1. The appropriate micro-step α_{μ} is calculated in accordance with the desired angular position resolution $\Delta\theta_{5d}$:

$$\alpha_{\mu} = \Delta\theta_{5d} \times K_{g5}. \quad (13)$$

2. The number of micro-steps k is defined on the basis of the α_{μ} value:

$$k = \alpha/\alpha_{\mu}. \quad (14)$$

3. The necessary phase current levels are calculated in compliance with Eqs. (9) and (10).

4. A respective lookup table for the microstepping mode of operation is compiled.

Theoretical and experimental research has been carried out for two-phase hybrid stepping motors with full motor step $\alpha = 1.8^\circ$.

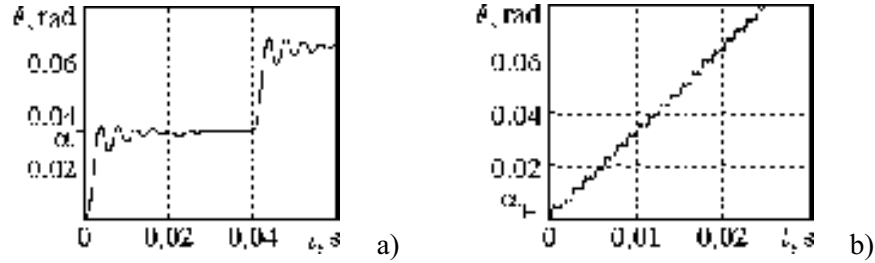


Figure 11: Full stepping (a) and microstepping mode (b).

Fig. 11 presents time-diagrams obtained for full stepping (a) and microstepping mode of operation (b) when one full step is divided into 8 substeps.

2.5. Spindle driving

Spindle driving must meet the following basic requirements:

- dual-zone speed regulation (by constant torque and constant power respectively);
- oriented braking with high accuracy;
- reversible speed control.

In the second zone the magnetic flux changes and to improve the electric drive performance an adaptive speed controller with switchable structure has been offered. In this zone the controller parameters adapt to the decreasing magnetic flux. Adaptation to flux change starts after the zone switching, which takes place at the specified base value of the armature voltage. Such an approach provides for better static and dynamic characteristics of the driving system.

The transfer function of the synthesized controller is described as follows [8]:

$$G_{sc}(s) = \frac{JK_{c1f}}{a_s K_{sf} \tau_{\mu s} c \Phi} \left(1 + \frac{1}{a_s^2 \tau_{\mu s}} \right) \quad (15)$$

where: J is total inertia referred to the motor shaft; K_{c1f} – gain of the armature current feedback; K_{sf} – gain of the speed feedback; c – motor coefficient; Φ – magnetic flux; a_s – coefficient influencing the speed loop dynamic characteristics; $\tau_{\mu s}$ – summary small time-constant, not subject to compensation.

Figure 12 presents angular speed oscilograms obtained experimentally for both zones of regulation. These time-diagrams are obtained for two reference motor speeds respectively: is 96 rad/s (Fig. 12a) and 144 rad/s (Fig. 12b).

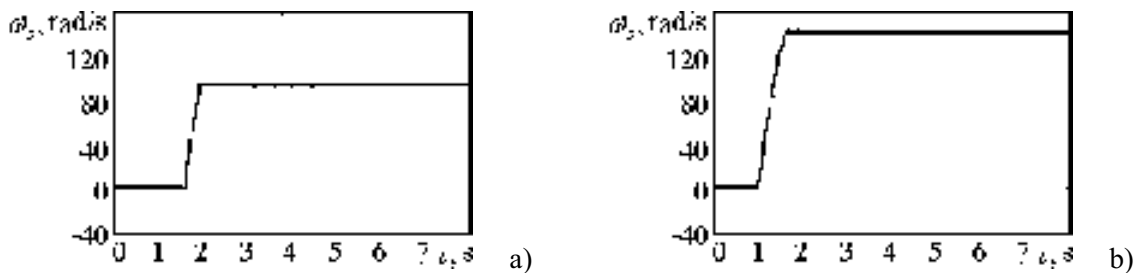


Figure 12: Speed oscilograms for both zones of regulation.

Figure 13 shows torque/speed characteristics of the spindle electric drive with dual-zone speed regulation, where ω_{\max} is the upper bound of the speed range and T_{\max} is the maximum motor torque. The speed zone switching is a function of the motor armature voltage.

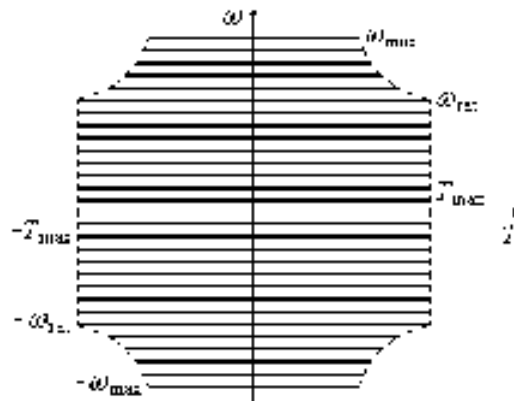


Figure 13: Torque/speed characteristics.

The motor speed is regulated at constant magnetic flux in the first zone, while in the second zone the flux is reduced at constant armature voltage. This way, speed control is realized at constant motor torque until the rated speed level ω_{rat} is reached. After that, it is carried out at constant power.

2.6. Coordination of the controlled axes

Appropriate software for digital program control has been developed to coordinate the all axes of the machine under consideration.



Figure 14: A machine part produced after the modernization.

Figure 14 presents a machine part produced after the milling machine modernization.

3. CONCLUSION

Modernization of a type of milling machines implementing two additional controlled axes has been realized. Better capabilities of these machines to process more complex machine parts are achieved, as well as increase of their productivity.

The requirements for static and dynamic characteristics of the respective coordinate axes have been formulated.

Models for computer simulation of electric drives with various algorithms for control have been developed.

Comparative analysis of different solutions with DC and AC motors has been carried out aiming at performance improvement.

Detailed experimental studies confirm good efficiency of the multi-coordinate driving system applied. The research carried out and results obtained can be used in the development and set up of such types of electric driving systems for machine tools.

4. ACKNOWLEDGEMENTS

This work has been supported by the Technical University of Sofia under Project No. 132PD0038-08/2013.

REFERENCES

- [1] Acarnley, P.: *Stepping Motors: a Guide to Theory and Practice*. London: IEE, 2002. ISBN 978-085-296-029-5.
- [2] Bose, B. K.: *Power electronics and motor drives: advances and trends*. London: Academic Press, 2006. ISBN 978-0-12-088405-6.
- [3] Hanselman, D.: *Brushless Permanent Magnet Motor Design*. Orono: University of Maine, 2006. ISBN 1-881855-15-5.
- [4] Keuchel, U., Stephan, R. M.: *Microcomputer-based adaptive control applied to thyristor-driven DC motors*. London: Springer-Verlag, 1994. ISBN 978-038-719-855-5.
- [5] Miller, T. J. E.: *Electronic control of switched reluctance machines*. Oxford: Newnes, 2001. ISBN 0-7506-50737.
- [6] Mohan, N.: *Electric drives – an integrative approach*. Minneapolis: MNPERE, 2003. ISBN 0-9715292-1-3.
- [7] Mikhov, M.; Zhilevski, M.: Options for Performance Improvement of Position Electric Drive for Milling Machines. *Proceeding of Technical University of Sofia*, Vol. 62, No. 2 (2012). pp. 268-278. ISSN 1311-0829.
- [8] Mikhov, M.; Zhilevski, M.: Computer Simulation and Analysis of Two-coordinate Position Electric Drive Systems. In: *Proceedings of the International Scientific Conference on Information, Communication and Energy Systems and Technologies*, Veliko Tarnovo, Bulgaria, 28-30. June 2012. Edited by Rumen Arnaudov. Sofia: Technical University of Sofia, 2012, pp. 251-254. ISBN 978-619-167-002-4.
- [9] Mikhov, M.; Zhilevski, M.; Spiridonov, A.: Modeling and Performance Analysis of a Spindle Electric Drive with Adaptive Speed Control, *Journal Proceedings in Manufacturing Systems*, Vol. 7, No. 3 (2012), pp. 153-158. ISSN 2067-9238.
- [10] Mikhov, M.; Zhilevski, M.: Analysis of a Multi-Coordinate Drive System Aiming at Performance Improvement. In: *Proceedings of the International Conference "Research and Development in Mechanical Industry"*, Vol. 1, Vrnjacka Banja, Serbia, 13-17. September 2012. Edited by Predrag Dašić. Vrnjacka Banja: SaTCIP Ltd., 2012, pp. 1102-1107. ISBN 978-86-6075-037-4.
- [11] Mikhov, M.; Zhilevski, M.: Introduction of additional coordinate axis in a class of machine tools with digital program control. *Proceeding of Technical University of Sofia*, Vol. 63, No. 2 (2013). pp. 41-48. ISSN 1311-0829.
- [12] Mikhov, M.; Balev, B.: Modeling and Optimization of an Electric Drive System with Dual-Zone Speed Regulation, In: *Proceedings of the International Scientific Conference on Information, Communication and Energy Systems and Technologies*, Nish, Serbia and Montenegro, June 29-July 01 2005, Edited by B. Milovanovic, Vol. 2, pp. 575-578, ISBN 86-85195-26-8.
- [13] Mikhov, M.; Georgiev, T.: An Approach to Synthesis of a Class of Electric Drives with Dual-Zone Speed Control, *Advances in Electrical and Computer Engineering*, Vol. 10, No. 4 (2010), pp. 87-94. ISSN 1582-7445.
- [14] Zhilevski, M.: Some problems in modernization of a class of milling machines. *Proceeding of Technical University of Sofia*, Vol. 63, No. 2 (2013). pp. 99-106. ISSN 1311-0829.
- [15] Mikhov, M.: Mathematical Modeling and Dynamic Simulation of a Class of Drive Systems with Permanent Magnet Synchronous Motors, *Applied and Computational Mechanics*, Vol. 3, No. 2 (2009), pp. 331-338. ISSN 1802-680X.
- [16] Mikhov, M.; Nakov, P.: Stepping Motor Drive for Precise Positioning Applications, In: *Proceedings of the International Scientific Conference on Information, Communication and Energy Systems and Technologies*, Nish, Serbia, 25-28. June 2008. Edited by Bratislav Milovanović. Nish: UNIGRAF, 2008, pp. 227-230. ISBN 978-86-85195-59-4.